An Intrinsic Carbon Nanotube Heterojunction Diode

Gabin Treboux,* Paul Lapstun, and Kia Silverbrook

Silverbrook Research, P.O. Box 207, Balmain 2041, NSW, Australia

Received: September 8, 1998; In Final Form: October 27, 1998

Carbon nanotubes are metallic, semimetallic, or semiconducting, depending on their helicity. This raises the possibility of forming nanoelectronic devices by joining tubes of differing helicity. We report calculations of the electronic properties of pairs of "armchair" and "zigzag" nanotubes joined linearly. The linear junction in each case consists of a nonalternant band of 5- and 7-membered rings. For a metal−semiconductor armchair−zigzag system, charge transfer from the armchair segment to the zigzag segment is calculated to occur. The distribution of electrostatic potentials seen by any electron transferred through the system is asymmetric along the tube axis, so the system is expected to exhibit rectifying behavior. The linear junction has specific electronic properties consistent with recent measurements of rectification in carbon nanotubes (Collins, P. G., et al. *Science* **1997**, *278*, 5335.

Carbon nanotubes have generated a great deal of interest since their discovery in 1991 by Iijima.[1] A wide variety of nanotube configurations has subsequently been experimentally observed, and theoretically and computationally analyzed. The strong interest in nanotubes stems from their extraordinary mechanical and electronic properties.

The geometrical structure of a single-wall nanotube (SWNT) is uniquely determined by the circumference vector $C = n\,a_1 + m\,a_2$, where a_1 and a_2 are graphene sheet lattice translation vectors. The (*n*,*n*) armchair nanotube, and the (*n*,*0*) zigzag nanotube both have a nonchiral configuration. The (*n*,*n*) armchair nanotubes are metallic while the (*n*,*m*) tubes are semimetallic if $n - m$ is a nonzero multiple of three, and semiconducting otherwise.[2]

Nanoscale electronic devices formed by joining nanotubes of differing helicity hold great promise. Several junctions which contain one or more pairs of 5- and 7-membered carbon ring defects have been proposed theoretically,[3−6] and experimental evidence of their occurrence in natural systems has been reviewed.[7]

However, many issues must be considered before such junctions can be designed for specific properties, even as a theoretical exercise. Here we consider a linear junction between an armchair and a zigzag nanotube.[6] This is a highly symmetric junction which consists of a circumference band of alternating 5- and 7-membered rings (Figure 1). In particular, we consider symmetry lowering at the junction, and the nonalternant nature of carbon nanotubes which incorporate 5- or 7-membered rings, which results in intrinsic charge separation.

Interestingly, the symmetry lowering and charge separation lead to specific conduction characteristics which are consistent with measurements reported by Collins et al.[8]

Symmetry Lowering

The symmetry of an infinite (*n*,*n*) armchair nanotube is D_{nh} where *n* is even, or D_{nd} where *n* is odd. An infinite (*m*,*0*) zigzag nanotube ($m = 2n$) is described by the symmetry group D_{mh}. Joining together the two nanotubes linearly lowers the symmetry of the whole system to C_{nv}. The first valence and conduction bands of the armchair segment belong to an *A* irreducible representation of the C_{nv} group, while the corresponding bands of the zigzag segment belong to an *E* representation (Figure 2).

Defining an angular momentum *L* with respect to the C_n axis, Chico et al.[6] showed that in terms of transport properties, such a symmetry difference leads to total reflection of the ballistic electron at the junction. The second valence and conduction bands of the armchair part belong to an *E* irreducible representation of the C_{nv} group, and ballistic transport is again possible.

Let us define *G* as the conductance of the system and *V* the voltage applied across it. The curve representing *G(V)* is then predicted to have a zero value in a window of width 2*W* centered at $V = 0$.

Using a tight-binding Hamiltonian of the form

$$H = \beta \sum_{ij} a_i^{\dagger} a_j + c.c. \tag{1}$$

where β is the nearest-neighbor hopping integral, W can be estimated for an (*n*,*n*) armchair tube by

$$W = -\beta \sin\left(\frac{(n-1)\pi}{n}\right) \tag{2}$$

if we neglect the shift of the second valence band induced by the junction.

The mismatch of the orbitals between the zigzag and the armchair nanotubes results in the loss of the first conductance channel, reducing the current in both directions. This could explain the 18-fold reduction in "forward" current seen between figures 3(C) and 3(D) of Collins et al.[8] Following the same argument, threshold conduction will occur at a voltage offset of *W* (as given by eq 2). With a value for the hopping integral β used by Chico et al.[4] (−2.66 eV), we calculate *W* to be 0.8 V for a (10,10)−(20,0) metal−semiconductor junction. It is interesting that Collins et al. report an offset of similar magnitude (0.5 V) in their SWNT experiments.

* Author to whom correspondence should be addressed. E-mail: gabin@silverbrook.com.au.

10.1021/jp983639m CCC: $18.00
Published on Web 02/27/1999

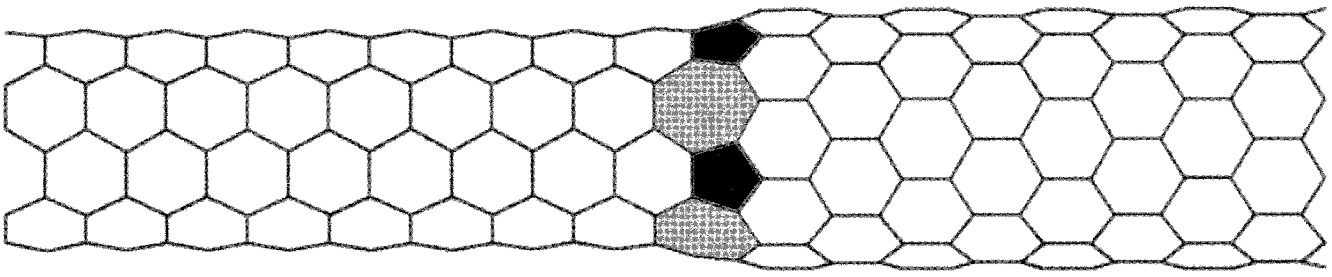

Figure 1. An armchair and a zigzag nanotube joined by a linear junction. The junction consists of a circumference band of alternating 5- and 7-membered rings.

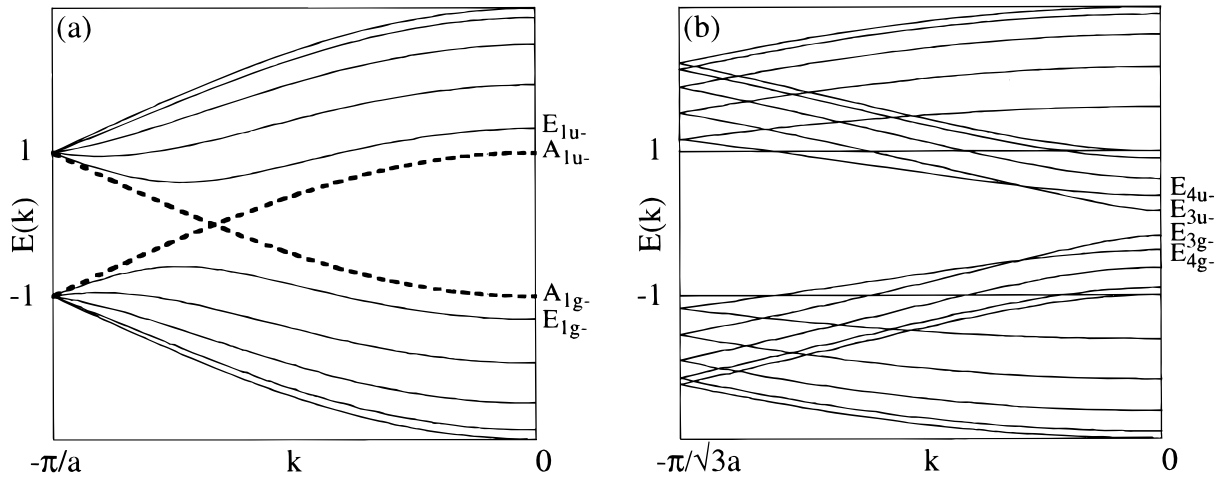

Figure 2. One-dimensional energy dispersion relations for a (5,5) armchair nanotube (a) and a (10,0) zigzag nanotube (b).[9] The energy is defined in terms of a unit nearest-neighbor hopping integral, and a is the lattice constant for the 2D graphene sheet. The first and second conduction and valence bands are labeled by the irreducible representations of the point group $D_{(2n+1)d}$ at $k = 0$.[9] The first valence and conduction bands of the armchair tube, shown dashed, cross at $k = -2\pi/(3a)$.

The symmetry mismatch affects conductance symmetrically. We now move on to consider a basis for asymmetric conductance.

Nonalternance

In alternant systems, the atoms can be divided into two distinct sets, no atom of one set being adjacent to an atom of the other.[10,11] Calling these atomic sets starred {*} and unstarred {0}, respectively, the bonding ψ_{l+} and antibonding ψ_{l-} orbitals of an alternant system occur in pairs with opposite energies, and can be written as

$$\psi_{l\pm} = \sum_i C_{li}\phi_i \pm \sum_j C_{lj}\phi_j \qquad (3)$$

so that the electron−hole density of states of the system is symmetric. In terms of chemical properties, a network of 6-membered carbon rings is alternant. In a nonalternant system, these two atomic sets cannot be defined, and eq 3 no longer applies. For instance, including 5- or 7-membered rings in a 6-membered ring network destroys the electron−hole symmetry, and the resulting system has carbon atoms bearing a net positive or negative charge.

The significance of this is that to achieve aromaticity, the 5-membered rings "borrow" π electron density from surrounding atoms, thus becoming negatively charged. Likewise, the 7-membered rings "donate" π electron density, thus becoming positively charged.

In the analysis of carbon nanotubes with homogeneous structure, the tight-binding Hamiltonian has proved to be usefully predictive[2] of experimental measurements.[12,13] However, here we are considering carbon nanotubes with heterogeneous structure, in which intrinsic charge separation occurs due to nonalternance. We therefore introduce a Hubbard electronic Hamiltonian, which includes an on-site electrostatic term:[14]

$$H = \beta\sum_{i,j} a^{\dagger}_i a_j + c.c. + U\sum_i n_{i,up}n_{i,down} \qquad (4)$$

The Hamiltonian is solved self-consistently using Hartree−Fock approximation. If we set U to zero we recover the tight-binding Hamiltonian.

The charge q_i on each atomic site is calculated according to Mulliken approximation and plotted as an s-like orbital representation:

$$q_i = 1 - \sum_j n_j c^2_{i,j} \qquad (5)$$

where n_j is the occupancy of the jth orbital. In Figure 3a,b we show the charge distribution for a (6,6)−(12,0) "metal−metal" linear junction calculated using the Hubbard Hamiltonian with $U = 0$ and $U = -2\beta$, respectively. It is well-known that increasing U beyond -2β leads to nonconvergence of the iterative self-consistent field (SCF) procedure.[15] The junction is connected to its mirror image to avoid end effects and the need for hydrogen termination.

Figure 3a shows that there is charge separation associated with the nonalternance of the system, as expected. Figure 3b shows that the inclusion of on-site electrostatic repulsion does not significantly damp the charge separation, even with a U value deliberately larger than that normally used with aromatic

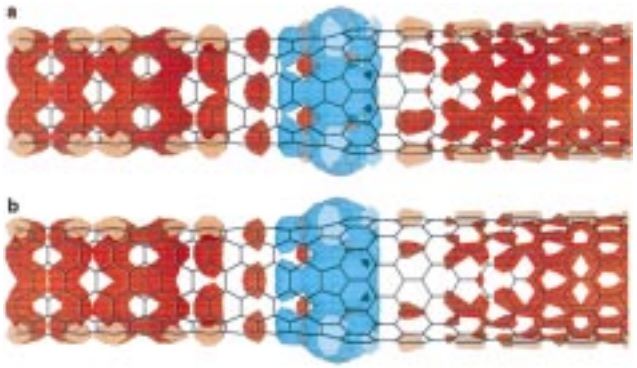

Figure 3. Charge distribution of the linear (6,6)−(12,0) metal−metal junction. Red indicates positive charge. Cyan indicates negative charge. Threshold = 0.0012 e/atom. Parameters: $\beta = -2.66$ eV. (a) $U = 0$. (b) $U = -2\beta$.

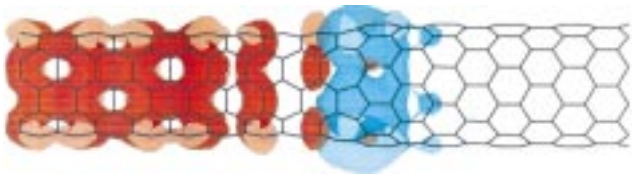

Figure 4. Charge distribution of the linear (5,5)−(10,0) metal−semiconductor junction. Red indicates positive charge. Cyan indicates negative charge. Threshold = 0.0012 e/atom. Parameters: $\beta = -2.66$ eV. $U = -2\beta$.

compounds.[16] The calculated charge separation is therefore not an artifact of the tight-binding model.

Figure 3 shows net negative charge on the 5-membered rings of the junction, and matching net positive charge distributed on both the armchair segment and the zigzag segment. The positive charge pattern on the armchair segment has the characteristic periodicity of the armchair Fermi wavelength.

In Figure 4 we show the charge distribution for a (5,5)−(10,0) "metal−semiconductor" linear junction calculated using the Hubbard Hamiltonian with $U = -2\beta$.

Figure 4 again shows that there is charge separation associated with the nonalternance of the system. The key feature of this metal−semiconductor system is that the positive charge is now located almost exclusively on the "metallic" armchair segment. Again we obtain very similar results with $U = 0$. Because the inclusion of an on-site repulsion term does not lead to qualitatively different results, we avoid the computational cost of the self-consistent procedure by using a tight-binding Hamiltonian ($U = 0$) in the remainder of this article.

To quantify the difference in behavior between the metal−metal system and the metal−semiconductor system, we consider inter-segment charge transfer, defined as the number of electrons which the armchair segment transfers to the zigzag segment.

The charge transfer is dependent on the respective lengths of the two segments. An infinitely long armchair nanotube has a metallic character while a finite tube has a metallic or semiconducting character, depending on its length.

There are three periodic situations as the length of the armchair tube is increased. In the first we have a junction in which the highest occupied molecular orbital (HOMO) and lowest unoccupied molecular orbital (LUMO) of the system are degenerate. In the second, an increase of the armchair length by half a circumference ring leads to a system with a band gap where the HOMO is of A_{1u} symmetry and the LUMO is of A_{1g} symmetry in point group D_{5d}. A further increase by half a circumference ring leads to the third situation, the reverse of the second, where the HOMO is of A_{1g} symmetry and the LUMO is of A_{1u} symmetry. These symmetry permutations simply trace out the valence and conduction band crossings of the infinitely long armchair nanotube (Figure 2). This band gap decreases with increasing nanotube length, converging to zero at infinity.

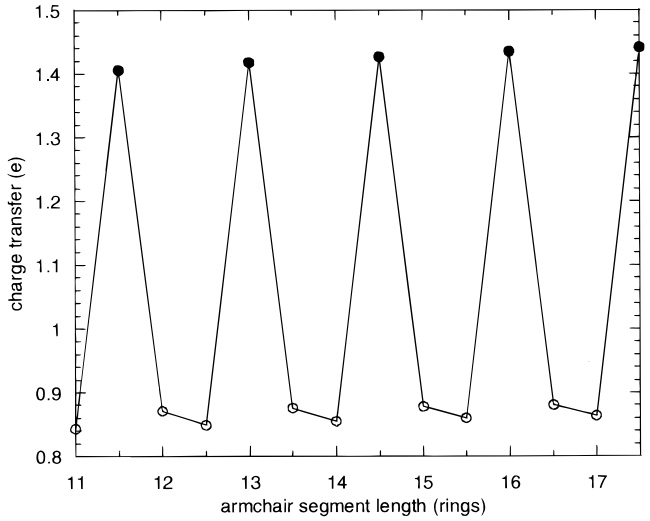

Figure 5. Charge transfer as a function of armchair segment length for a linear (5,5)−(10,0) junction. The zigzag segment length is fixed at 31 circumference rings. The armchair segment oscillates between zero band gap metallic character (filled circles) and semiconductor character (open circles). Parameters: $\beta = -2.66$ eV. $U = 0$.

An infinitely long zigzag nanotube has a metallic or semiconductor character depending on its circumference index. A finite length zigzag tube has localized states at both ends of the tube. At the tight-binding level, these states are at zero energy and so give the tube a metallic character independent of its circumference index. These states do not correlate with the first valence and conduction bands of the corresponding infinitely long nanotube, but instead correlate with the bands of zero dispersion at $E = \beta$ (see Figure 2b). We therefore still classify a finite length zigzag tube according to the metal-semiconductor character of its corresponding infinitely long tube, and define its band gap as the energy difference between the first valence and conduction energy levels which correlate with the first valence and conduction bands of the corresponding infinitely long tube.

If we connect a finite armchair tube to a finite semiconductor zigzag one, we find two distinct regimes. When the armchair band gap is larger than that of the zigzag segment, we obtain the charge-transfer curve of Figure 5. The periodic metal−semiconductor character of the armchair segment is apparent.

When the armchair segment is longer, its band gap is smaller than that of the zigzag, and charge transfer from the higher-energy armchair side to the lower energy zigzag side is stabilized. The length at which the regime changes is circumference dependent, since the band gap of the semiconductor zigzag segment decreases with increasing circumference. For a (5,5)−(10,0) system it occurs at an armchair segment length of 17.5 rings. We then obtain the charge-transfer curve of Figure 6, where the same periodic oscillation is seen, but with amplitude 2 orders of magnitude smaller. The normalization condition applied to the orbitals explains the decrease in modulation amplitude with increasing length.

If we connect a finite armchair tube to a finite metallic zigzag tube, both band gaps decrease with increasing tube length. As they converge on zero, the basis for the charge transfer disappears. When the two segments have a similar finite length,

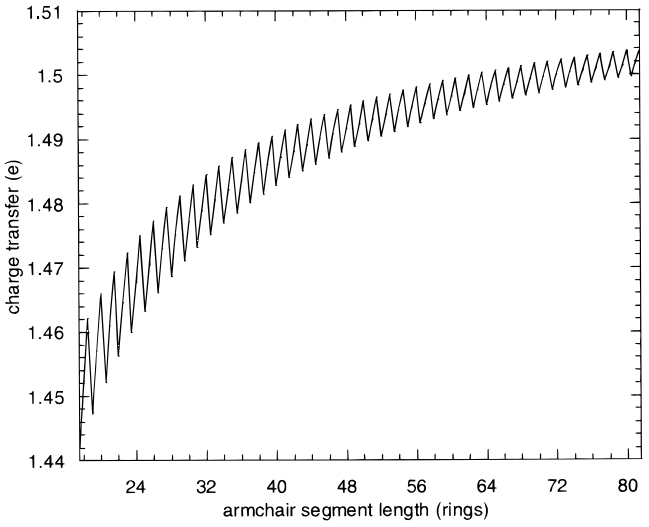

Figure 6. Charge transfer as a function of armchair segment length for a linear (5,5)−(10,0) junction, for lengths greater than those in Figure 5. The zigzag length is fixed at 31 circumference rings. Parameters: $\beta = -2.66$ eV. $U = 0$.

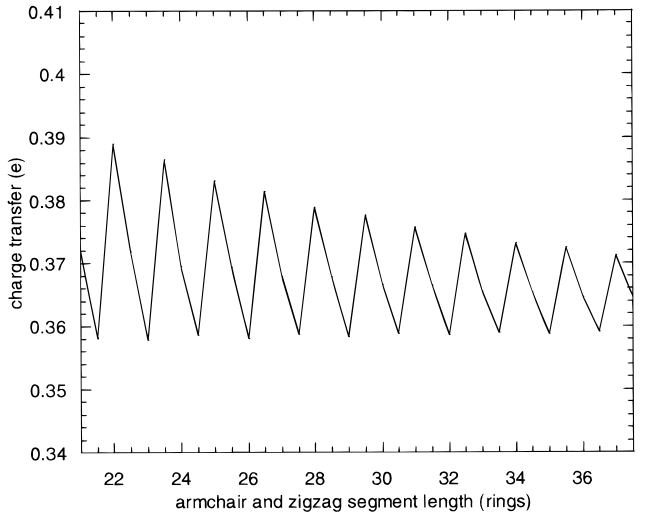

Figure 7. Charge transfer as a function of segment length for a linear (6,6)−(12,0) junction. The armchair and zigzag segment lengths are identical. Parameters: $\beta = -2.66$ eV. $U = 0$.

the band gaps are misaligned, but only by a small amount (<0.02 eV). This is overpowered by kT at room temperature. Assumption of a Fermi−Dirac electron distribution leads at room temperature to the charge-transfer curve of Figure 7.

Rectification

The ballistic conductance of the system can be analyzed using the Landauer formalism. If the voltage is measured by a noninvasive four-probe apparatus, this will give the intrinsic conductance of the junction. Experimentally, however, the conductance is usually measured where the tube is between a conductive substrate and the sharp tip of a scanning tunneling microscope.[8] In such a two-probe measurement the conductance is a characteristic of the whole system, including the substrate/tube interface, the internal tube junctions, and the tube/tip interface. In this case the following formula applies:[17]

$$g = \frac{2e^2}{\pi\hbar} Tr(t^\dagger t) \tag{6}$$

where t is the transmission coefficient. Here we implicitly have

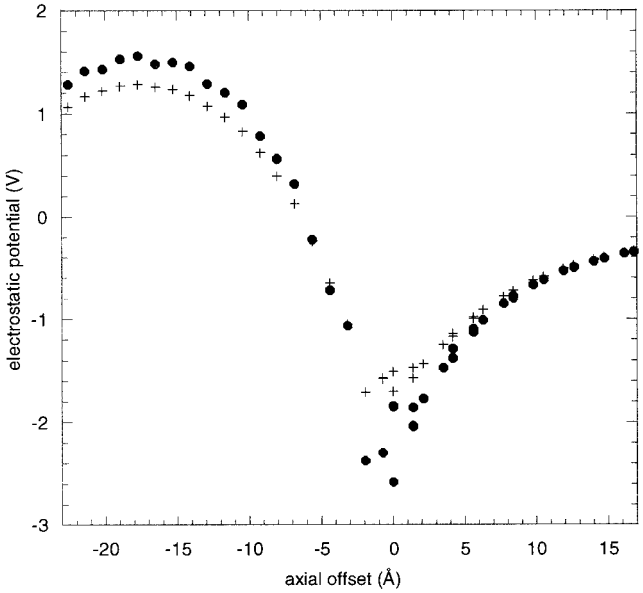

Figure 8. Axial distribution of electrostatic potentials (V) calculated at every atomic site of the (5,5)−(10,0) junction shown in Figure 4. The junction edge of the zigzag segment is at the origin. Each potential value is calculated at a fixed distance of 1 Å (filled circles) and 2 Å (crosses) from an atomic site, along the convex surface normal. Due to the circumferential symmetry of the system, only two distinct values are seen within each curve at each axial offset. Parameters: $\beta = -2.66$ eV. $U = -2\beta$.

to take into account the voltage drops at the interfaces and junction when calculating the *I/V* curve.

A number of two-probe measurements of molecular rectification have been reviewed.[18] The systems can be classified into three categories: D-σ-A molecules[19] (where D and A represent the donor and acceptor parts), D-π-A zwitterionic molecules,[20] and π molecules asymmetrically placed between the two probes.[21] We recognize a fourth category, where nonalternance leads to intrinsic charge separation and rectification.[22] Following this argument, the charge separation calculated for the metal−semiconductor junction presented in this article should create an asymmetry in its *I/V* curve, i.e., the junction should exhibit rectifying behavior.

To obtain a rough estimate of the electrostatic potential associated with this charge distribution we use a classical expansion to calculate ϕ_i at a point i using the charge calculated using the Hubbard Hamiltonian:

$$\phi_i = \sum_j \frac{q_j}{4\pi\epsilon_0 r_{ij}} \tag{7}$$

In Figure 8 we show the electrostatic potential of the metal−semiconductor system presented in Figure 4. Each potential value is calculated at a fixed distance of both 1 and 2 Å from an atomic site, along the convex surface normal.

Due to the circumferential symmetry of the system, only two distinct electrostatic potential values are possible within each curve at each axial offset. In fact, it is only at the junction that the two values are significantly different. Figure 8 shows that the calculated charge distribution leads to a significant potential difference between the armchair and zigzag segment in the vicinity of the junction.

Discussion

We have presented calculations of the charge distribution in a nonalternant system consisting of an armchair and a zigzag

nanotube joined by a linear junction. In the case of a metal−semiconductor junction we have reported a large axial asymmetry in the charge distribution, specifically a charge transfer from the armchair segment to the zigzag segment. This large axial asymmetry suggests that the system may operate as a rectifier. The difference in behavior between the metal−metal junction and the metal−semiconductor junction reported here supports the notion that a metal−semiconductor system provides the basis for a nanoelectronic device, as first put forward by Saito.[23]

We are currently developing more quantitative methods to refine the results presented in this article. This includes a multireference representation of the wave function of the metal system calculated at the Hubbard level, and connecting the system to theoretical electrodes to study the voltage dependence of the charge separation.

The concept of asymmetry can be applied to any carbon network containing 5- and 7-membered rings, so such systems should in principle exhibit some rectification. We have performed similar calculations on various metal−semiconductor nanotube heterojunctions proposed by others. These include an (8,8)−(14,0) "knee" junction formed by opposing 5- and 7-membered rings;[3] an (8,0)−(7,1) junction formed by a single transversely aligned 5−7 defect;[4] and a (12,0)−(11,0) bill-like junction formed by a single axially aligned 5−7 defect.[5] These systems exhibit much weaker charge separation and do not have a nonconduction region associated with symmetry mismatching. At the level of our calculations, these systems therefore less adequately explain the experimental results of Collins et al.[8]

It remains an open question whether the highly symmetric linear junction considered here could have been present in the SWNT mat in which Collins et al.[8] found the rectifier. Certainly the spontaneous synthesis of a linear junction in a carbon arc seems highly improbable if one assumes that the junction is formed by random defects in a continually growing nanotube. An alternative view is that the junction is formed when the open ends of two growing nanotubes come close enough to join. We would be very interested in experimental evidence of such block copolymerization.

In the experimental results obtained by Collins et al.[8] the conductance of the system fell abruptly to zero a short distance from the location of the rectifier. This could be explained if the tip were to come to the end of the nanotube at this time. However, it could also be explained by the presence of a pair of rectifiers arranged back-to-back.[24] Linear junctions may frequently occur in pairs, if the nanotubes were to form by block copolymerization of armchair and zigzag fragments, and if one nanotube type were more prevalent than the other. Such a structure may be analogous to a bipolar junction transistor if a "base" connection is made between the opposing junctions.

Whatever the interpretation of the results of Collins et al.[8] finally turns out to be, it is clear that the linear junction is a potential candidate for nanoelectronic devices.

References and Notes

(1) Iijima, S. *Nature* **1991**, *56*, 354.
(2) Saito, R.; Fujita, M.; Dresselhaus, G.; Dresselhaus, M. S. *Appl. Phys. Lett.* **1992**, *60*, 2204.
(3) Lambin, Ph.; Fonseca, A.; Vigneron, J. P.; Nagy, J. B.; Lucas, A. A. *Chem. Phys. Lett.* **1995**, *245*, 85.
(4) Chico, L.; Crespi, V. H.; Benedict, L. X.; Louie, S. G.; Cohen, M. L. *Phys. Rev. Lett.* **1996**, *76*, 971.
(5) Charlier, J. C.; Ebbesen, T. W.; Lambin, Ph. *Phys. Rev. B* **1996**, *53*, 11108.
(6) Chico, L.; Benedict, L. X.; Louie, S. G.; Cohen, M. L. *Phys. Rev. B* **1996**, *54*, 2600.
(7) Ebbesen, T. W. *Carbon Nanotubes − Preparation and Properties*; Ebbesen, T. W., Ed.; CRC Press: Boca Raton, FL, 1997.
(8) Collins, P. G.; Zettl, A.; Bando, H.; Thess, A.; Smalley, R. E. *Science* **1997**, *278*, 5335, 100.
(9) Dresselhaus, M. S.; Dresselhaus, G.; Eklund, P. C. *Science of Fullerenes and Carbon Nanotubes*, Academic Press: New York, 1996; p 805.
(10) Coulson, C. A.; Rushbrooke, G. S. *Proc. Camb. Philos. Soc.* **1940**, *36*, 193.
(11) Longuet-Higgins, H. C. *J. Chem. Phys.* **1950**, *18*, 265.
(12) Wildoer, J. W. G.; Venema, L. C.; Rinzler, A. G.; Smalley, R. E.; Dekker, C. *Nature* **1998**, *391*, 59.
(13) Odom, T. W.; Huang, J.-L.; Kim, P.; Lieber, C. M. *Nature* **1998**, *391*, 62.
(14) Hubbard, J.; *Proc. R. Soc. London Ser. A* **1963**, *276*, 238.
(15) Koutecky, Y.; Bonacic, V. *J. Chem. Phys.* **1971**, *55*, 2408.
(16) Malrieu, J. P.; Maynau, D. *J. Am. Chem. Soc.* **1982**, *104*, 3021.
(17) Landauer, R. *J. Phys.: Condens. Matter* **1989**, *1*, 8099.
(18) Roth, S.; Blumentritt, S.; Burghard, M.; Cammi, E.; Carroll, D.; Curran, S.; Dusberg, G.; Liu, K.; Muster, J.; Philipp, G.; Rabenau, T. *Synthetic Metals* **1998**, *94*, 105.
(19) Aviram, A.; Ratner, M. A. *Chem. Phys. Lett.* **1974**, *29*, 277.
(20) Martin, S.; Sambles, J. R.; Ashwell, G. J. *Phys. Rev. Lett.* **1993** *70*, 218.
(21) Roth, S.; Blumentritt, S.; Burghard, M.; Fisher, C. M.; Muller-Schwanneke, C.; Muster, J.; Philipp, G. In *Atomic and Molecular Wires*; Joachim, C., Roth, S., Eds.; Kluwer: Dordrecht, 1997.
(22) Treboux, G.; Lapstun, P.; Silverbrook, K. *J. Phys. Chem. B* **1998**, *45*, 8978.
(23) Saito, R.; Dresselhaus, G.; Dresselhaus, M. S. *Phys. Rev. B* **1996**, *53*, 2044.
(24) Collins, P. G.; Bando, H.; Zettl, A. Fifth Foresight Conference on Molecular Nanotechnology, Palo Alto, Oct. 1997.